

Microphysical evidence of the transition between predominant convective/stratiform rainfall associated with the intraseasonal oscillation in the Southwest Amazon.

Rachel Ifanger ALBRECHT¹; Maria Assunção Faus da SILVA DIAS¹

ABSTRACT

The distinction between convective and stratiform precipitation profiles around various precipitating systems existent in tropical regions is very important to the global atmospheric circulation, which is extremely sensitive to vertical latent heat distribution. In South America, the convective activity responds to the Intraseasonal Oscillation (IOS). This paper analyzes a disdrometer and a radar profiler data, installed in the Ji-Paraná airport, RO, Brazil, for the field experiment WETAMC/LBA & TRMM/LBA, during January and February of 1999. The microphysical analysis of wind regimes associated with IOS showed a large difference in type, size and microphysical processes of hydrometeor growth in each wind regime: easterly regimes had more turbulence and consequently convective precipitation formation, and westerly regimes had a more stratiform precipitation formation.

KEYWORDS

intraseasonal oscillation, drop size distribution, precipitation, profiler radar, disdrometer.

Evidência microfísica da transição entre períodos convectivos e estratiformes associados à oscilação intrasazonal na região sudoeste da Amazônia.

RESUMO

A diferenciação entre os perfis de precipitação convectiva e estratiforme dentre os diversos sistemas de precipitação existentes na região tropical é muito importante para a circulação atmosférica global, sendo extremamente sensível à distribuição vertical de calor latente. Na América do Sul, a atividade convectiva responde à Oscilação Intrasazonal (IOS). Este trabalho analisa dados de um disdrômetro e um radar de apontamento vertical instalados no aeroporto de Ji-Paraná, RO, Brasil, para o experimento de campo WETAMC/LBA & TRMM/LBA, em Janeiro e Fevereiro de 1999. A breve análise dos regimes de ventos associados à IOS mostrou um grande diferença no tipo, tamanho e processos microfísicos de crescimento de hidrometeoros em cada regime de vento: regimes de leste possuem mais turbulência e conseqüentemente formação de precipitação convectiva, e regimes de oeste possuem formação de precipitação mais estratiforme.

PALAVRAS-CHAVE

oscilação intrasazonal, distribuição de tamanho de gotas, precipitação, radar de apontamento vertical, disdrômetro.

INTRODUCTION

The global atmospheric circulation is sensitive to the vertical distribution of latent heating, which is associated with different types of precipitation (Kasahara and Silva Dias, 1986; DeMaria, 1985). Therefore, it is important to distinguish between convective and stratiform precipitation profiles around various precipitating systems observed in tropical regions (Garstang *et*

al., 1994; Garreaud e Wallace, 1997; Carvalho *et al.* 2002). In South America, the high variability of convective activity and intense precipitation is related to some aspects of global atmospheric circulation, in particular to the Intraseasonal Oscillation, IOS (Kousky and Kayano, 1994; Jones and Carvalho, 2002). The IOS is related to a systematic eastward movement

¹Departamento de Ciências Atmosféricas - Universidade de São Paulo. Rua do Matão, 1226 - São Paulo, SP - CEP 05508-090

of low-frequency large-scale convection and circulation anomalies along the equatorial belt, for a period of 20 to 60 days (Madden e Julian, 1994). The classical definition of *monsoon* is a seasonal reversal of large scale circulation due to differential heating of continents and oceans (Zhou e Lau, 1998). The dominant seasonal feature of the monsoon systems is the division of the seasons into 'wet' and 'dry'. These refer respectively to periods of high precipitation, when humid oceanic winds blow into the continent, and periods of reversed winds that drive cold and dry air from the center of winter continents. The variability of the South American summer monsoon, associated with the IOS, stimulates changes in low level winds and convective activity for periods of some days to weeks or more (Zhou e Lau, 1998). During the monsoon wet season, there are several variations in large scale patterns, like a short period of drought associated with the IOS. The drought period is denominated as the inactive phase of the monsoon system, or 'break monsoon', while the other periods are referred to as the active phase.

During the South American summer, an anticyclonic circulation at the upper troposphere, known as the Bolivian High, is followed by a trough in the east, which extends over the western Atlantic Ocean known as the Northeast Brazilian trough (Kousky and Gan, 1981). In low levels, a continental low pressure center of heat develops over Gran Chaco in Argentina. This low level atmospheric circulation pattern has a northwesterly flow along the eastern Andes in the tropics and subtropics, and a predominant east-northeasterly flow over the Amazon basin, accompanied by intense convective activity and precipitation. Kousky (1979) observed that the slow-moving cold fronts and subtropical upper tropospheric cyclonic vortices play an important role in characterizing the precipitation over Brazil. These quasi-stationary fronts are referred to as the South Atlantic Convergence Zone (SACZ, Nobre, 1988), and is recognized as one of the main features of the wet season (Silva Dias and Marengo, 1999).

As previous studies suggested that the characterization of the low level jets in South America is due to baroclinic systems, recent authors have studied the connection between SACZ (which is associated to IOS) and convection over the Amazon, using data collected during the WET Atmospheric Mesoscale Campaign (WETAMC) and Tropical Rainfall Measuring Mission (TRMM) field experiments in Rondonia (southwest Amazonia), Brazil, as part of the Large-scale Biosphere Atmosphere experiment in Amazonia (LBA) (Herdies *et al.*, 2002; Rickenbach *et al.*, 2002; Halverson *et al.*, 2002; Carvalho *et al.*, 2002; Tokay *et al.*, 2002; Albrecht and Pereira Filho, 2002; Silva Dias *et al.* 2002; Pereira Filho *et al.* 2001). This field experiment took place in January and February of 1999 and

collected a unique data base with high temporal and spatial resolutions of synoptic, meso and micro-scales features of the atmosphere and its precipitation characteristics. The experiment set up, localization and instrumentation are described in Silva Dias *et al.* (2002). Rickenbach *et al.* (2002) observed that, during this experiment, the zonal wind alternated its direction from east to west at low and middle troposphere. These periods may be seen in Table 1. They also computed the displacement of cold fronts observed during that experiment, and found that the presence of stationary cold fronts for several consecutive days was associated with periods of more intense westerlies (W1 e W3), suggesting a strong correlation between westerly flow over Southwest Amazon and SACZ characterization. Therefore, the wind regime periods were classified as "non-SACZ" (E1, E2, E3 and W2) and "SACZ" (W1 and W3) periods. Rickenbach *et al.* (2002) also analyzed precipitation estimatives of a radar placed in Rondonia and observed that during "non-SACZ" regimes there were smaller convective systems in horizontal extension with more convective fraction of precipitation, while during "SACZ" periods there was 27% less precipitation mainly due to the weak intensity of convective systems, but they had approximately twice the horizontal extension of "non-SACZ" systems. This difference in precipitation is attributed to the IOS, which modulates the SACZ.

Tokay *et al.* (2002) analyzed data from two disdrometers installed in the WETAMC/LBA experiment area and compared them with data collected in Darwin, Australia. This region has the same Amazonian wind regime characteristics, which is a classic monsoon (westerlies) and break (easterlies) regimes. The mean drop size distribution based on Darwin and Rondonia wind regimes showed more large drops in easterlies (break monsoon) and more small drops during westerlies (monsoon).

This difference in number of drops is associated with the origin of precipitation in mesoscale convective system (MCS) patterns for each wind regime period: easterlies have more

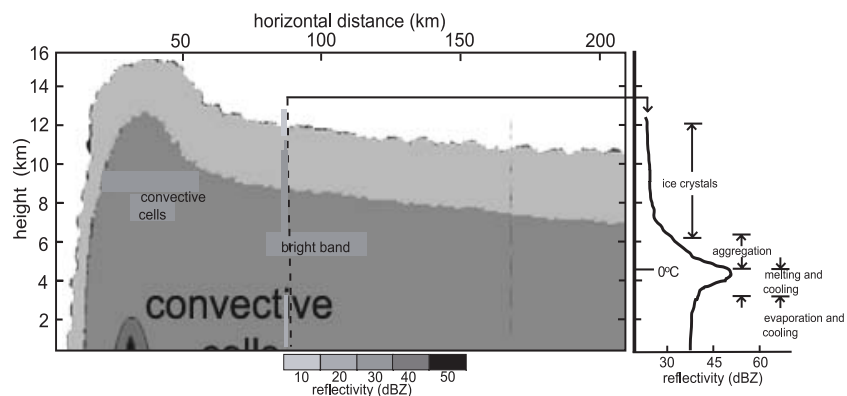


Figure 1 - A transversal mesoscale convective system (MCS) reflectivity section scheme. The anvil is near the intense convective cells and extends horizontally in a stratiform precipitation region. The vertical reflectivity profile indicates the microphysical processes involved in stratiform precipitation. Adapted from Williams *et al.* (1995).

convective precipitation and westerlies have more stratiform precipitation from the MCSs. The microphysical distinction between stratiform and convective precipitation lies on the magnitude of in cloud vertical motions. Stratiform precipitation occurs when the vertical velocity in the cloud (w) does not exceed the terminal fall velocity of ice crystals and snow ($v_{ice} = 1 - 3 \text{ ms}^{-1}$), or $|w| < v_{ice}$ (Houze, 1993). At upper levels of stratiform clouds, ice particles grow mainly by vapor deposition, and when they have enough mass to not be sustained by vertical motions, they start to fall slowly, and then, grow by aggregation and rimming around 2.5 km above the 0°C level. Below the height of 0°C isotherm, ice particles melt and this level is easily identified by a horizontal bright band radar echo with a thickness of 500 m (Fabry e Zawadzki, 1995; Gage *et al.*, 1996). These processes are illustrated in Figure 1.

Convective processes are quite different from the stratiform ones. Vertical motions are about 1 to 10 ms^{-1} or more, which equals or exceeds terminal fall velocities of ice crystals and snow (Houze, 1993). Therefore, particles grow by rimming and are carried up and down inside the cloud by up and downdrafts. Because updrafts exist in a limited region of the convective clouds, radar echoes associated with active convection form a vertical region of maximum reflectivity, which contrasts with the horizontal orientation of radar bright band seen in the melting layer of stratiform precipitation (Figure 1).

Several authors suggested that the period when the WETAMC/LBA & TRMM/LBA experiment took place is a period driven by IOSs, characterizing a monsoon regime similar to those found in Asia (Petersen *et al.*, 2001). In this paper we describe the relation between the variability of large scale flow patterns over South America and changes in microphysical properties of Southwest Amazon local convection, as a result of IOSs. Synoptic characteristics of the transition between break and monsoon regimes can be easily detected by the zonal wind and outgoing long wave radiation data, while microphysical characteristics of this transition need a more detailed analysis of the precipitation processes involved. Therefore, a brief synoptic description of January and February of 1999 is shown as well as a microphysical description of the whole period, and two case studies using data from a profiler radar and an impact disdrometer, specially placed in Rondônia for the WETAMC/LBA & TRMM/LBA experiment.

Table 1 - Periods defined by the lower troposphere zonal flow, where "E" indicates east flow, "W" indicates west flow, and SACZ and non-SACZ indicate periods of a well and a non-well, respectively, established South Atlantic Convergence Zone. Adapted from Rickenbach *et al.* (2002).

Period	Date
E1 - "non-SACZ"	11/Jan to 13/Jan
W1 - "SACZ"	14/Jan to 18/Jan
E2 - "non-SACZ"	19/Jan to 28/Jan
W2 - "non-SACZ"	29/Jan to 07/Feb
E3 - "non-SACZ"	08/Feb to 21/Feb
W3 - "SACZ"	22/Feb to 01/Mar

DATA AND METODOLOGY

The dataset used to describe the synoptic features of the WETAMC/LBA & TRMM/LBA experiment consists of the GPSA (Global Pacific South America) CPTEC (Centro de Previsão de Tempo e Clima) grid analysis of zonal and meridional winds. The microphysical features were studied by a 915 MHz (33 cm wavelength) Doppler profiler radar and a Joss-Waldvogel impact disdrometer, both placed at the Ji-Paraná airport, Rondonia, within a distance of a few meters. The period analyzed is from January 17th to March 2nd, 1999 and it is divided into 5 sub periods based on Table 1.

The profiler radar measures the three moments of Doppler spectrum: reflectivity (Z - proportional to the sixth power of the drop diameter distribution within the volume sample), Doppler velocity (V) and spectral width (SW - which is a measure of the turbulence within the volume sample). It operates in 105 and 210 m of resolution, with a frequency of one profile per minute, and a vertical range of 10 km and 19 km, respectively. The Joss-Waldvogel disdrometer (JWD) measures the number of drops that are stored into 20 size intervals ranging from 0.36 to about 5.4 mm for 1 minute period. This instrument was originally designed to calculate the radar reflectivity factor (Z) and has some limitations: it cannot measure drops smaller than 0.36 mm and larger than 5.4mm; it underestimates the number of small drops in heavy rain; and its calibration assumes that the drops are falling at terminal velocity in still air.

The daily mean, maximum and standard deviation of the three Doppler spectral moments, and the daily mean diameter weighted by the number of drops have been calculated to analyze the general characteristics of the precipitation systems. Only volume samples with $Z > 0 \text{ dBZ}$ where considered in the analysis of the profiler radar data to avoid, in a simple way, clear air echoes.

The more specific characteristics of the precipitation systems have been studied by focusing on two MCS that occurred on January 26th and February 24th, 1999. These MCSs have been qualitatively analyzed by some infrared GOES-8 images, vertical profiles of profiler radar, and JWD data.

JANUARY-FEBRUARY 1999 SYNOPTIC CONTEXT

To better illustrate the synoptic context of the WETAMC/LBA & TRMM/LBA experiment, the patterns of mean wind flow in the lower (850 hPa) and upper (200 hPa) troposphere, for periods of "SACZ" (predominance of westerlies) and "non-SACZ" (predominance of easterlies) in Table 1, are found in Figure 2 and Figure 3. These figures clearly show that periods of westerlies had a northeastern flow from the Equatorial Atlantic Ocean to the middle latitudes in 850 hPa (characterizing the low level jet), and there was the presence of the Bolivian High at 200 hPa and a well defined cyclonic vortex of the Northeast Brazil over the Western Tropical Atlantic. During periods of low level easterlies, it was observed that the easterly wind flow at 850 hPa over the Amazon Basin, and the northeastern flow observed in the other case were restricted to the proximity of

the Andes' slope, while the Bolivian High was well defined at 200 hPa, as well as the upper level trough (Northeast Brazilian Trough). Therefore, the more evident differences were found at low level flow. Figure 4 reinforce the presence of zonal winds at 850 hPa mainly from the west during "SACZ" periods and from the east during "non-SACZ" for the radiosonde site Fazenda Nossa Senhora (11°S, 62°W). It can be noticed that the W2 period did not have strong westerlies, therefore it did not characterize a typical westerly regime.

MYCROPHYSICAL CHARACTERISTICS

In a preliminary analysis the daily mean variables of the profiler radar and JWD were used. Figure 5 shows the mean-weighted daily diameters in respect to the total number of drops by each diameter interval measured by the JWD, located at Ji-Paraná airport. This figure shows that easterly periods had drops with larger diameters since mean weighted diameter is about 0.5 and 1.5 mm, while for the westerly case drops diameter is from 0.5 to just 1.0 mm. This is evidence of a convective feature for easterly regime.

Figure 6 and Figure 7 show the daily mean variables measured by the profiler radar featuring, in a generic way, periods of westerlies and easterlies. Figures 6a and 6b show that the daily mean reflectivity and its standard deviation had its highest values over the region of 2 to 8 km, that is, the region where liquid water and ice were present. The highest *in situ* values of mean reflectivities are at ~ 5 km height, where the 0°C isotherm is localized and, consequently, the radar bright band associated to the melting of falling ice particles (Section 1, Figure 1). It is noted that the radar bright band was present in both wind regimes, but it was more evident in easterly regimes, except for the W3 period. However, westerly regimes had low standard deviation for profiler radar variables (inclusive W3), while easterly regimes had the highest standard deviations, which is coherent with the fact that there were fewer systems with small horizontal extensions than in westerlies. This standard deviation behavior shows the homogeneity of westerly regimes. A notably fact in the reflectivity standard deviation is the region between 9 and 12 km height: high standard deviations are observed, but the respective mean is very low. This is explained by the maximum reflectivities observed at this

same region in Figure 6e, which is associated with noise clearly seen at the instantaneous one minute reflectivity profiles (not shown). This fact hides the maximums associated with the radar bright band.

Analyzing the mixed phase of hydrometeors (3.5 to 6.5 km), it is observed that the highest values of mean reflectivity (Figures 6c and 6f) are concentrated around the radar bright band, and in the case of easterlies these values are relatively in higher positions, up to 6.5 km (Figure 6f).

Figure 7 shows daily mean profiles of vertical Doppler velocity and spectral width (related to the turbulence). It can be seen that the daily mean velocity was more positive for easterly regime and its standard deviation was very high, indicating the presence of strong updrafts (Figures 7a and 7b). The turbulence was concentrated below the 0°C isotherm during westerly regimes, but during the easterly regime it

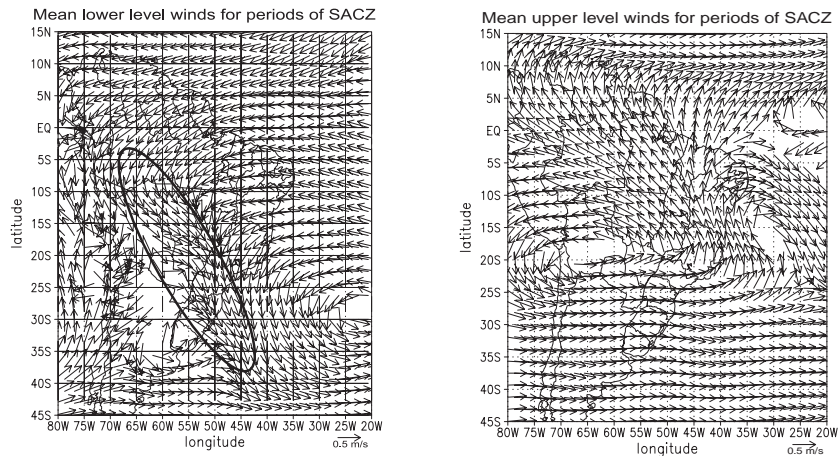


Figure 2 - (a) Low level, 850 hPa, and (b) high level, 200 hPa, mean wind for regimes defined by SACZ (Table 1). GPSA CPTEC analysis. The area indicated in (a) corresponds to the SACZ.ab

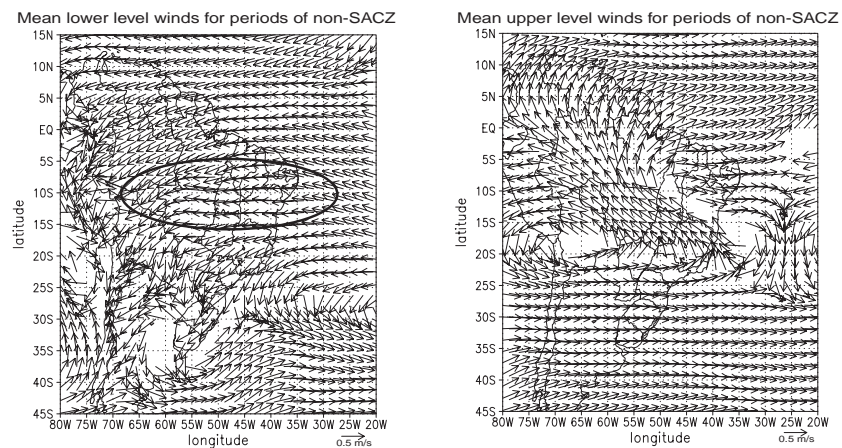


Figure 3 - (a) Low level, 850 hPa, and (b) high level, 200 hPa, mean wind for regimes defined by non-SACZ (Table 1). GPSA CPTEC analysis. Easterlies are indicated in (a).

exceeded this height due to strong convection (Figure 7c), related to the strong up and downdrafts.

January 26th: An easterly case study

The January 26th squall line moved through the experiment area from northeast to southwest with high rainfall rates at its leading edge, and moderate stratiform rainfall at its trailing edge. Animation of satellite imagery showed that this squall line probably originated from an organized convection initiated at the Northeastern Brazilian coast and traveled hundreds of kilometers reaching the Rondonia state.

This squall line had a slow displacement with a large convective area that lasted for more than 2 hours while moving over the experiment area, as can be inferred by the very cold cloud tops in Figure 8. The very convective feature of this

squall line can be verified by Figure 9. There is a great number of middle to large sized drops in the beginning of the squall line life cycle, when it passed over the disdrometer at 2030 UTC. By 2115 UTC the squall line convective leading edge moved southwest of Ji-Paraná airport and just the stratiform trailing edge of this system was detected: small drops of ~ 1 mm until the end of precipitation.

The precipitation processes that originated drops detected by the disdrometer can be inferred by profiler data shown in Figure 10. The first hour of heavy precipitation with a great number of large drops was mainly convective, with high values of reflectivity ($Z > 50$ dBZ) from the ground to around 7 km height. These high values of reflectivity were accompanied by strong downdrafts under 6 km in height, and also a mixture of strong downdrafts and some updrafts above this height, due to the very strong turbulence caused by convection. The strong turbulence causes very high values of spectral width in this region. The microphysical processes of convective precipitation is the accretion of liquid water to small size drops as they are carried to upper and lower levels by the up and downdrafts, since this is the only way fast enough to allow particles to develop quickly (Houze, 1993). After the first hour of precipitation, the drops were small and their vertical reflectivity profiles had a well defined radar bright band, which is due to the melting of ice particles falling over the 0°C isotherm. This type of precipitation came from the trailing edge of the MCS and from its decaying stage. This MCS had the same structure as illustrated in Figure 1.

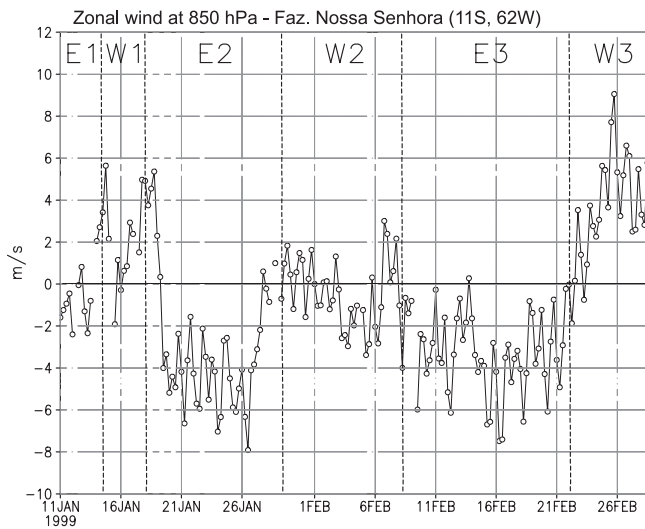


Figure 4 - Zonal wind at the pressure level of 850 hPa. over radiosonde site Fazenda Nossa Senhora (11°S, 62°W), during WETAMC/LBA experiment. Dashed lines separate and indicate beginning/end of zonal Wind periods from Table 1.

February 24th: A westerly case study

The February 24th system had a long life (~ 5 hours) and a very slow displacement from east to west over the experimental area. It had just a few convective cells as shown by the mainly relatively warm tops in the infrared satellite images (Figure 11). The disdrometer first detected its precipitation to be around 1130 UTC and it was composed just by some small drops. By 1330 UTC, the precipitation rate increased by a large number of small and middle sized drops.

The precipitation processes that originated drops detected by the disdrometer can be inferred by the profiler data shown in Figure 12. During the first two hours of the MCS, there was a well defined radar bright band, but disappeared around 1230 UTC. Around 1345 UTC hydrometeors were detected above 6 km height; it is the formation of ice particles mainly by vapor deposition and rimming. Some time after this, the radar bright band, with $Z \sim 35$ dBZ, was well defined by the ice particles falling through the melting level to the ground at a not so high velocity, and starting to grow also by aggregation. At this time, around 1415 UTC, middle sized drops were detected by the disdrometer and reflectivity from this period had a slanted profile reinforcing the slow decaying particles. This feature lasted for more than two hours. The spectral width profile had small values during the whole period, indicating that there was no convective activity involved.

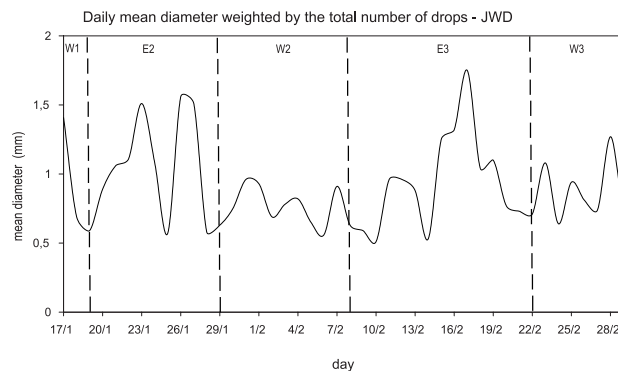


Figure 5 - Daily mean diameter weighted by the total number of drops. Dashed lines separate and indicate beginning/end of zonal Wind periods from Table 1ab

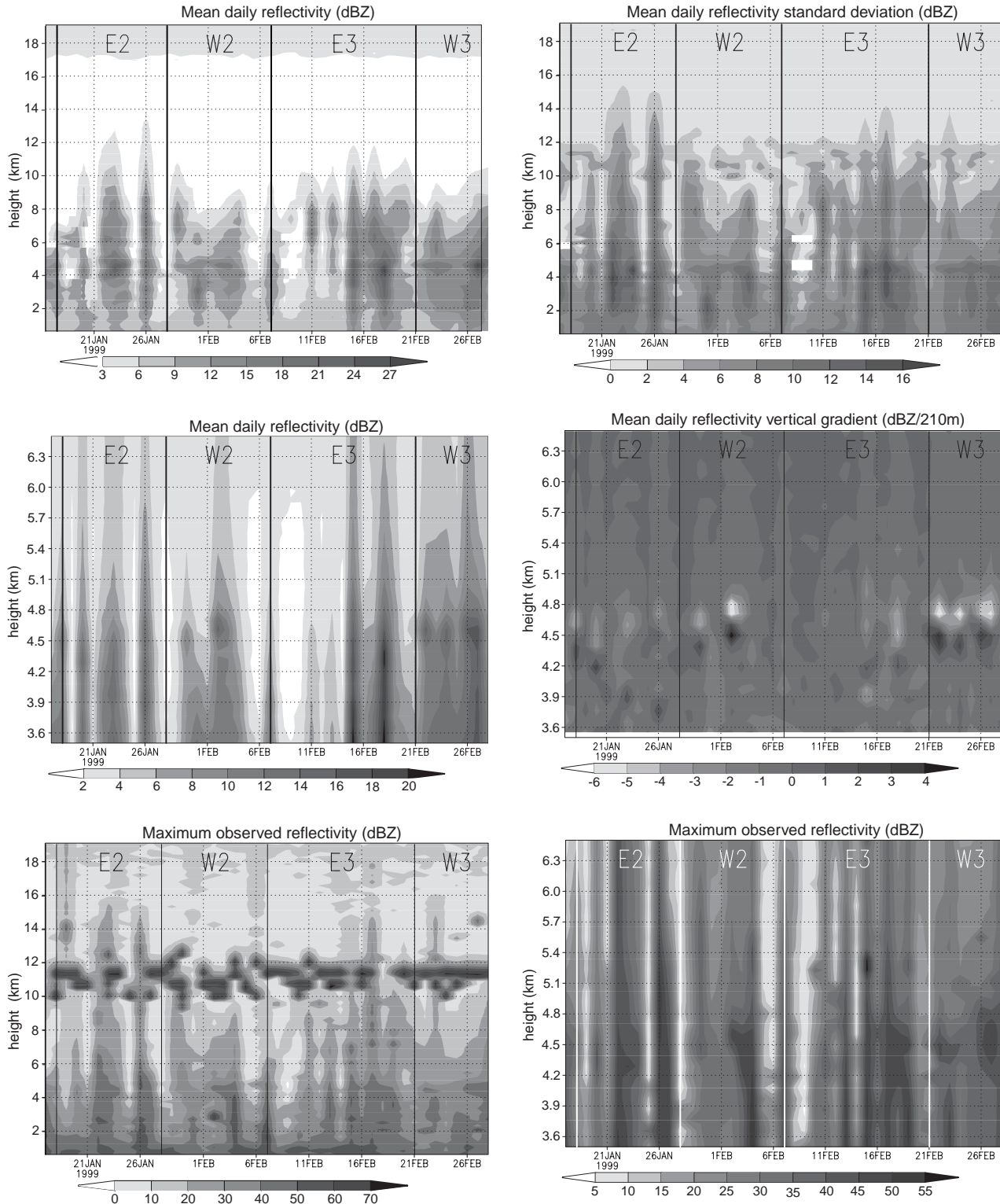


Figure 6 - (a) Daily mean reflectivity, (b) daily mean reflectivity standard deviation, (c) daily mean reflectivity over mixed phase region (3.5 to 6.5 km), (d) vertical daily mean reflectivity gradient over mixed phase region, (e) maximum reflectivity observed, and (f) maximum reflectivity observed over mixed phase region. E2, W2, E3 and W3 indicate periods of east and west winds (Table 1). Only values with $Z > 0$ dBZ were considered.

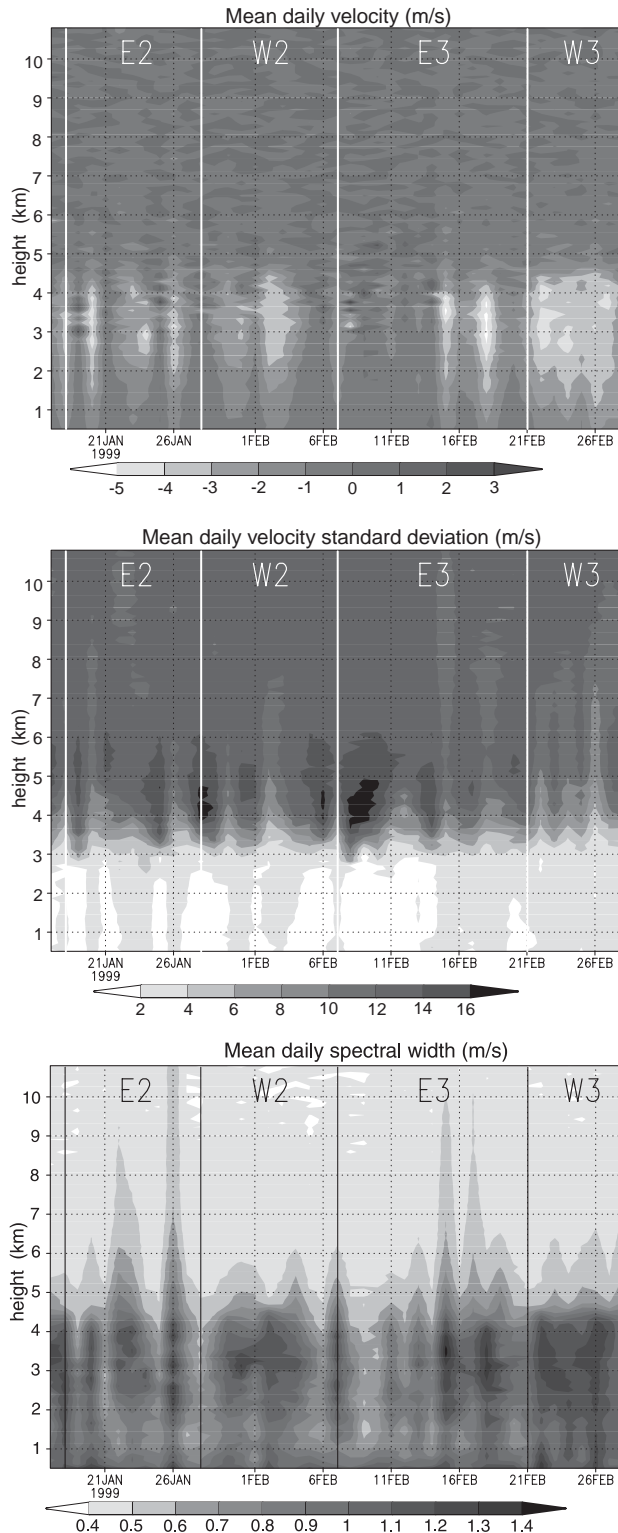


Figure 7 - (a) Daily mean Doppler velocity, (b) daily mean Doppler velocity standard deviation, and (c) daily mean spectral width. E2, W2, E3 and W3 indicate periods of east and west winds (Table 1). Only values with $Z > 0$ dBZ were considered.

DISCUSSION AND CONCLUSION

Through the analysis of the disdrometer and profiler radar, it was possible to analyze the detailed microphysical structure related to a more convective pattern of easterly regimes and a more stratiform pattern of westerly regimes, associated with the intraseasonal oscillation present during the WETAMC experiment. The brief microphysical analysis of convective regimes associated with the IOS showed a large difference in type, size and microphysical processes of hydrometeor growth in each wind regime. Specially, the weak vertical reflectivity gradient around 0°C isotherm, combined with the high values of reflectivity and vertical velocity over this same region, suggests the presence of large particles inside the entire convective structure of the easterly wind regime systems. The strong updrafts in the MCS events in the easterly wind regime, as observed on January 26th MCS and also reported by Cifelli *et al.* (2002), suggest that a considerable number of drops were carried above the melting level, representing an important source of large ice particles and supercooled drops in this region. In westerly regimes, the ice particles were mainly small ice crystals and snow, and the drops were small, as was observed on the February 24th MCS. This difference in hydrometeor profile is mainly due to the strong spectral width observed during easterly regimes and the weak ones observed during westerly regimes (Figure 7). Strong spectral width is due to convective precipitation formation mechanisms (turbulence), allowing particles to rapidly grow by accretion of liquid water, while weak spectral width is due to weak turbulence, which allows ice particles to grow by deposition of vapor water, aggregation and, in a last way, by accretion.

The presence of hydrometeors in high levels affects the vertical distribution of the electric activity of the system, as was verified by Petersen *et al.* (2002) for the period studied (there is a larger electric activity in easterly wind regimes). But the main effect is the large latent heating source at upper levels, which affects the propagation of upper level waves and interhemisphere teleconnections. This is very important to weather and climate prediction models (Kasahara and Silva Dias, 1986). The microphysical and large scale analysis of the precipitating system during WETAM/LBA & TRMM/LBA experiment indicate a relationship between the variability of large scale flow patterns over South America and changes in the microphysics of convection over the Southwest Amazon.

ACKNOWLEDGMENTS

Thanks to Dr. Carlos Morales and Dr. Ali Tokay for their useful discussions on the microphysics of precipitation and disdrometer data, Dr. Augusto Pereira Filho for his cooperation, and FAPESP (Fundação de Apoio à Pesquisa do Estado de São Paulo) for the research assistantship grant, number 01/11532-6. Parts of this work were funded by FAPESP, CNPq, NASA (TRMM and LBA) and the European Community (SMOCC).

LITERATURE CITED

Albrecht, R. I.; Pereira Filho, A. J. 2002: Temporal evolution of ZR relationships over precipitating systems during WET-AMC/LBA and TRMM/LBA, *Second International Scientific LBA Conference, Manaus – AM*, July 07-10 2002.

Carvalho, L. M. V.; Jones C.; Silva Dias, M. A. F. 2002: Intraseasonal large-scale circulations and mesoscale convective activity in tropical South America during the TRMM-LBA campaign. *J. Geophys. Res.*, 107(D20): doi 10.1029/2001JD000745.

Cifelli, R.; Petersen, W. A.; Carey, L. D.; Rutledge, S. A.; Silva Dias, M. A. F. 2002: Radar observations of the kinematic, microphysical, and precipitation characteristics of two MCSs in TRMM-LBA., *J. Geophys. Res.*, 107(D20): doi 10.1029/2000JD000264.

DeMaria, M. 1985: Linear response of a stratified tropical atmosphere to convective forcing. *J. Atmos. Sci.*, 42: 1944-1959.

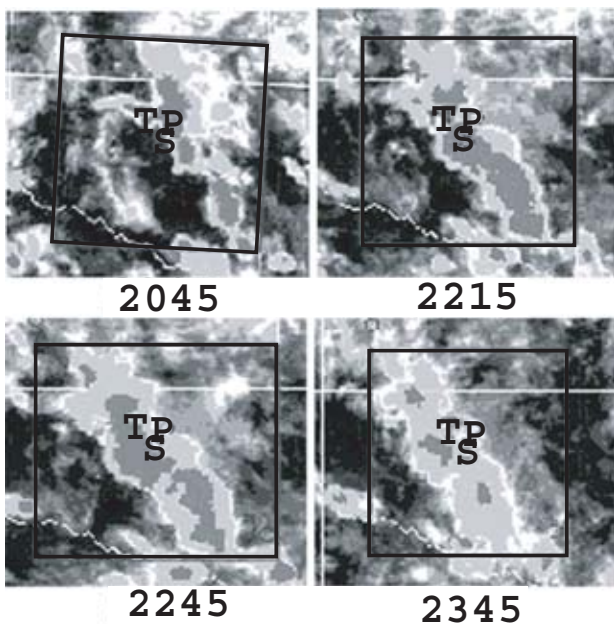


Figure 8 - January 26th, 1999 channel 4 GOES satellite images for times indicated in UTC. Rectangle indicates the WETAMC/LBA experiment area, S – S-Pol radar, T – TOGA radar, and P – profiler radar. Cloud colors go from white to dark gray (colder tops).

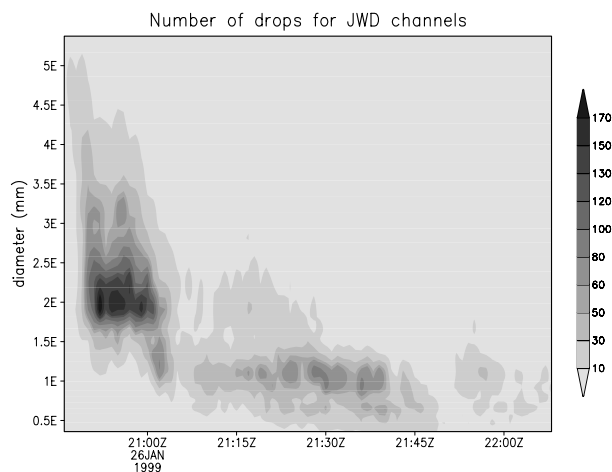


Figure 9 - January 26th, 1999 rain drop spectrum evolution.

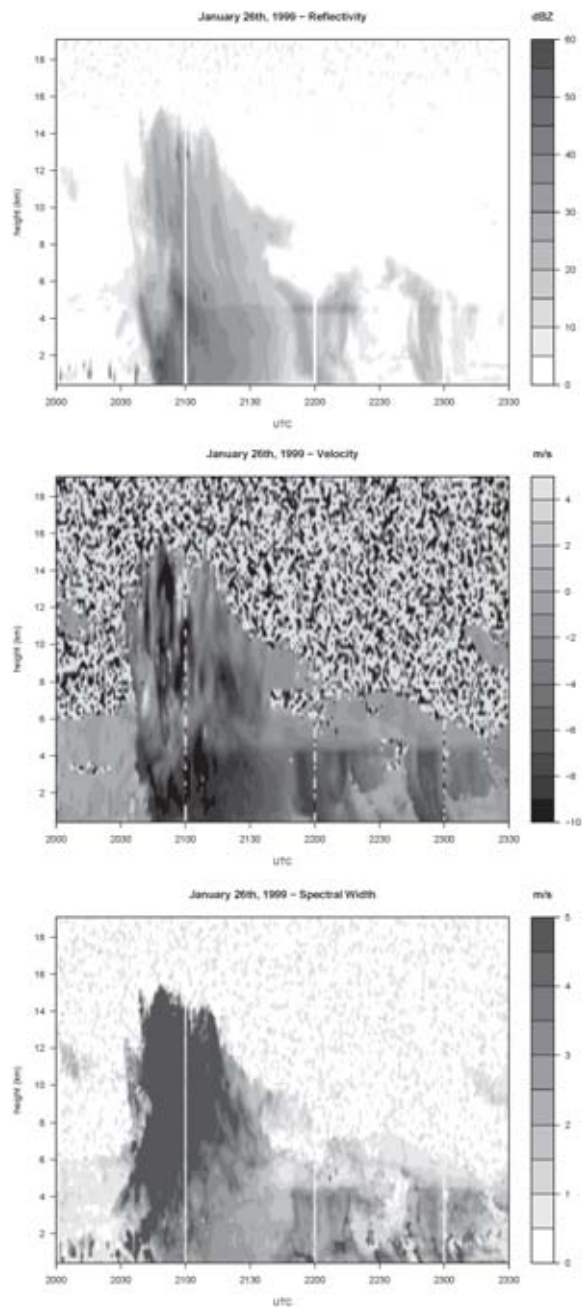


Figure 10 - January 26th, 1999 profiler radar variables: (a) reflectivity, (b) Doppler velocity, and (c) spectral width.

Fabry, F.; Zawadzki, I. 1995: Long-term radar observations of the melting layer of precipitation and their interpretation. *J. Atmos. Sci.*, 52: 838-851.

Gage, K. S.; Williams, C. R.; Ecklund, W. L. 1996: Application of the 915MHz profiler for diagnosing and classifying tropical precipitation cloud systems. *Meteorol. Atmos. Phys.*, 59: 141-151.

Gargstang, M.; Massie Jr., L.; Halverson, J.; Greco, S.; Scala, J. 1994: Amazon coastal squall lines, Part I, Structure and kinematics. *Mon. Weather Rev.*, 122: 608-622.

Garreaud, R. D.; Wallace, J. M. 1997: The diurnal march of convective cloudiness over the Americas, *Mon. Weather Rev.* 125: 3157-3171.

Halverson, J. B.; Rickenbach, T. M.; Roy, B.; Pierce, H.; Williams, E. 2002: Environmental characteristics of convective systems during TRMM-LBA. *Mon. Wea. Rev.*, 130: 1493-1509.

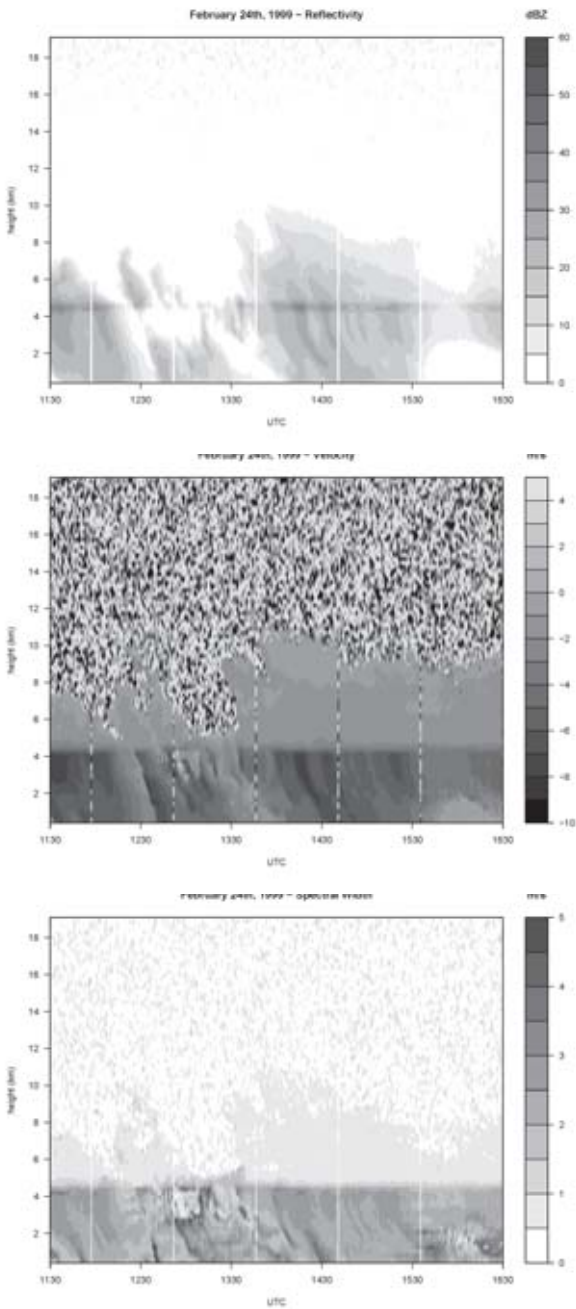


Figure 13 - February 24th, 1999 profiler radar variables: (a) reflectivity, (b) Doppler velocity, and (c) spectral width.

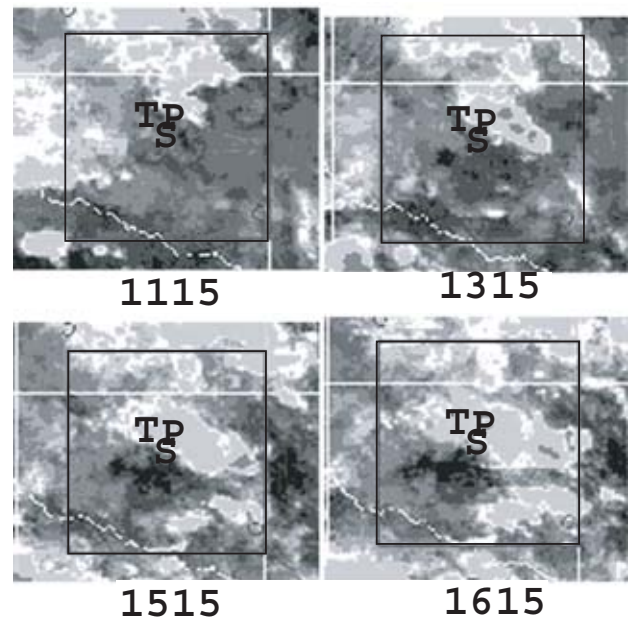


Figure 11 - February 24th, 1999 channel 4 GOES satellite images for times indicated in UTC. Red rectangle indicates the WETAMC/LBA experiment area, S - S-Pol radar, T - TOGA radar, and P - profiler radar. Cloud colors go from white to dark grey (colder tops).

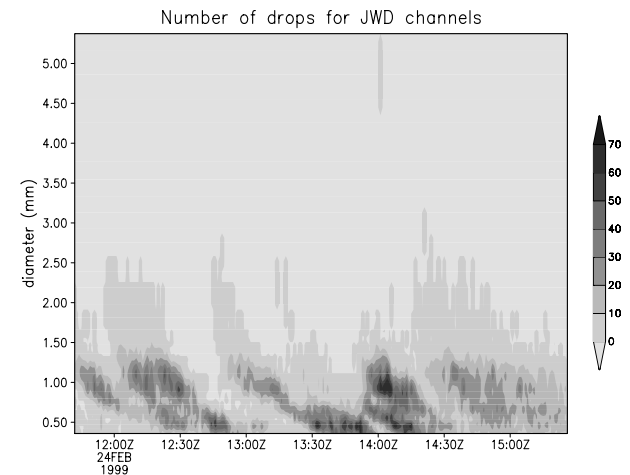


Figure 12 - February 24th, 1999 rain drop spectrum evolution.ab

- Herdies, D. L.; da Silva, A.; Silva Dias, M. A. F. 2002: The bi-modal pattern of the summertime circulation over South América. *J. Geophys. Res.*, 107(D20): doi: 10.1029/2001JD000337.
- Houze, R. A. 1993: Cloud Dynamics. *Academic Press*, 573pp..
- Jones, C.; Carvalho, L. M. V. 2002: Active and break phases in the South American monsoon system. *J. Climate*, 15: 905-914.
- Kasahara A.; Silva Dias, P. L. 1986: Response of planetary waves to stationary tropical heating in a global atmosphere with meridional and vertical shear. *J. Atmos. Sci.*, 43 (18): 1893-1911
- Kousky, V. E. 1979: Frontal influences on northeast Brazil. *Mon. Wea. Rev.*, 107: 1140-1153.
- Kousky, V. E.; Gan, M. A. 1981: Upper tropospheric cyclonic vortices in the tropical South-Atlantic. *Tellus*, 33 (6): 538-551 1981
- Kousky, V. E.; Kayano, M. T. 1994: Principal modes of outgoing longwave radiation and 250-mb circulation for the South American sector. *J. Climate*, 7: 1131-1143.
- Madden, R. A.; Julian, P. R. 1994: Observation of the 40-50 day tropical oscillation - A Review. *Mon. Wea. Rev.*, 122: 814-837.
- Nobre, C 1988: Ainda sobre a Zona de Convergência do Atlântico Sul: A importância do Oceano Atlântico. *Climanálise*, 3(4), 30-33.
- Pereira, A. J.; Albrecht, R. I.; Tokay, A. 2001: S-Pol measurements and DSD estimates of reflectivity during the WET-AMC/LBA and TRMM/LBA experiment in Rondônia, Brazil, *30th International Conference on Radar Meteorology, AMS, Munich, Germany*, July 2001.
- Petersen, W. A.; Nesbitt, S. W.; Blakeslee, R. J.; Cifelli, R.; Hein, P.; Rutledge, S. A. 2001: TRMM observations of convective regimes in the Amazon. *J. Clim.*, in press.
- Rickenbach, T. M.; Nieto Ferreira, R.; Herdies, D. L.; Silva Dias, M. A. F.; Halverson, J. 2002: Modulation of convection in the Southwestern Amazon Basin by extratropical stationary fronts. *J. Geophys. Res.*, 107(D20): doi: 10.1029/2001JD000334.
- Silva Dias, M. A. F.; Rutledge, S.; Kabat, P.; Silva Dias, P. L.; Nobre, C.; Fisch, G.; Dolman, A. J.; Zipser, E.; Garstang, M.; Manzi, A.; Fuentes, J. D.; Rocha, H.; Marengo, J.; Plana-Fattori, A.; Sá, L.; Alvalá, R.; Andreae, M. O.; Artaxo, P.; Gielow, R.; Gatti, L. 2002: Clouds and rain processes in a biosphere-atmosphere interaction context in the Amazon region. *J. Geophys. Res.*, 107(D20): doi 10.1029/2001JD000335.
- Silva Dias, P. L.; Marengo, J. 1999: Águas atmosféricas. *In: Águas Doces do Brasil. Ed. IEA/ABC*, p. 65-115.
- Tokay, A.; Kruger, A.; Pereira, A. J. 2002: Measurements of drop size distributions in Southwestern Amazon Basin. *J. Geophys. Res.*, 107(D20): doi 10.1029/2001JD000355.
- Zhou, Z; Lau, K.-M. 1998: Does a monsoon climate exist over South America? *J. Climate*, 11: 1020-1040.

**RECEBIDO EM 29/10/2003
ACEITO EM 17/05/2005**